Measurements of Critical Gradient Behavior of Fast-Ion Transport from Alfvén Eigenmodes for Predictive Model Development*

C.S. Collins[1], W.W. Heidbrink[2], M. Podestà[3], R.B. White[3], G.J. Kramer[3], D.C. Pace[1], C.C. Petty[1], L. Stagner[2], M.A. Van Zeeland[1], Y. B. Zhu[2], and the DIII-D team

[1] *General Atomics, PO Box 85608, San Diego, CA 92186-5608, USA*

[2] *University of California at Irvine, Irvine, CA 92697, USA*

[3] *Princeton Plasma Physics Laboratory, PO Box 451, Princeton, NJ 08543-0451, USA*

Abstract. Experiments in the DIII-D tokamak show that many overlapping small-amplitude Alfvén eigenmodes (AEs) cause fast-ion transport that is consistent with the critical gradient paradigm. Measurements indicate a sudden increase in fast-ion transport in the presence of many simultaneous AEs at a threshold in neutral beam power corresponding to a threshold for orbit stochasticity [1]. The threshold varies in fast-ion phase space and is well above the AE linear stability threshold, meaning that some AEs can be tolerated before performance-degrading transport occurs. Above threshold, transport becomes stiff, resulting in virtually unchanged fast-ion density profiles despite increased beam drive. These studies are being used to develop a validated, predictive transport model that can efficiently calculate AE-induced transport and the resulting fast-ion profile over a wide parameter regime in order to design optimal fusion reactor scenarios that avoid undesirable AE-transport.

I. Critical Gradient Experiments and Modeling

Experiments were conducted in the current ramp phase of a DIII-D inner wall limited, oval-shaped, low-confinement (L-mode) plasma with reversed-shear magnetic safety factor (q) profile. Total AE activity increased with neutral beam injected (NBI) power, and a mix of both frequency sweeping reversed-shear Alfvén eigenmodes (RSAEs) and near-constant frequency toroidicity induced Alfvén eigenmodes (TAEs) were observed. The bulk fast-ion distribution and instability behavior was also manipulated with varied beam deposition geometry. Additional experiment details can be found in [2]. To measure transport, the fast-ion pressure profile was modulated using an off-axis neutral beam, and a variety of fast-ion diagnostics were used to measure the fast-ion density evolution. A novel analysis uses the linearized continuity equation to solve for the divergence of modulated fast-ion flux, $\nabla \cdot \tilde{\Gamma}$, which is non-zero if AE's transport fast-ions into or out of the unique region of phase space measured by each diagnostic [3].

Since AEs can perturb a portion of fast-ion phase space while leaving other parts unaffected, the measured transport threshold varies between fast-ion diagnostics that are sensitive to different regions in phase space. The NPA diagnostic is sensitive to a narrow range of trapped particles with energies $\sim$40-80 keV, while the neutron signal is broadly sensitive to the high energy fast ions over a large volume. In Fig. 1a-b, the neutral particle analyzer (NPA) measures

a rise in transport above ∼4 MW beam power, while the neutron diagnostic measures the onset of transport at a much lower beam power.

Theoretical analysis shows that the measured onset threshold for fast-ion transport corresponds to the threshold in the number of fast-ion orbits that become stochastic after interaction with AEs [1, 2]. To calculate stochasticity, eigenmode solutions are first found with the ideal MHD code NOVA and compared to experimental data at a single timeslice, using magnetics to determine toroidal mode number and coherent AE-induced electron cyclotron emission (ECE) temperature fluctuations to scale mode amplitude. The scaled NOVA modes are used as input to the guiding center code ORBIT to determine which orbits have good Kolmogorov-Arnold-Moser (KAM) surfaces and which orbits become stochastic due to AEs. Figure 1c compares stochastic orbits for two different NBI geometries in the NPA region of phase space. The tangential NBI case #159243 had 8 RSAEs and 3 TAEs, resulting in a large number of stochastic orbits (red dots inside of yellow box), while the perpendicular NBI case #162753 had comparatively fewer modes (5 RSAEs and 3 TAEs) at lower amplitudes, resulting in a fewer number of stochastic orbits (blue dots inside of black box). In Fig. 1d, the sum of the stochastic orbits in the NPA region is plotted vs. beam power. No significant differences in the threshold for the onset of stochastic orbits occurs, in good agreement with the measured threshold results in Fig. 1b.

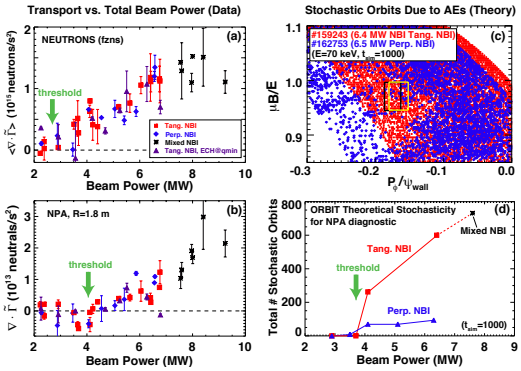

Figure 1: *The transport threshold is lower for (a) neutrons than for (b) the NPA diagnostic. (c) AE's cause orbits to become stochastic in the NPA region of phase space, and (d) the stochastic threshold is similar for different NBI geometries.*

Time-dependent TRANSP simulations using the kick model [5] accurately reproduce the measured signals (Fig. 2) and further reveal that it is not straightforward to do quantitative comparisons of the inferred transport measurements because the linear assumption that the source of modulated particles is constant in time no longer holds [2, 4]. In Fig. 2c, the model shows that the majority of the response in the data signals is due to transport of the steady (non-modulated) beam particles, which become modulated because the modulated NBI also modulates the AE amplitude. This nonlinearity affects the inferred transport levels in two ways. First, even though overall AE amplitude is lower in perpendicular NBI compared to tangential NBI, the modulated beam creates similar levels of modulated AE amplitude, which ends up

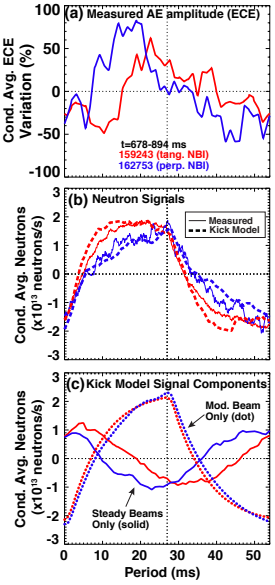

Figure 2: *(a) Modulated NBI injection modulates AE amplitude. (b) Simulations match neutron signals and reveal (c) the majority of signal distortion is due to transport of steady beams.*

transporting similar levels of background beam particles. Second, during the first half of the beam modulation period, the AE amplitude grows earlier in the perpendicular NBI case. This causes the fast-ion data signal to decay earlier, resulting in an amplified level of inferred transport relative to the tangential NBI since the time-average of the divergence of flux is taken over the same latter portions of the half period.

II. Electron Cyclotron Heating Alters AE Activity and Losses

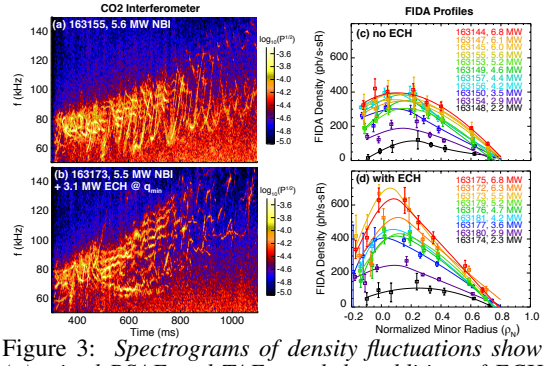

Figure 3: *Spectrograms of density fluctuations show (a) mixed RSAE and TAEs, and the addition of ECH results in (b) mainly TAEs. (c) FIDA profiles become stiff with increased beam power, and (d) reach higher density when ECH is added.*

The addition of electron cyclotron heating (ECH) changes the types of AEs present, increases the measured fast-ion density, and alters loss behavior. In Fig. 3, the tangential beam power scan was repeated with 3.2 MW of radially launched, 110 GHz ECH power deposited near $q_{\min}$. This results in a TAE-dominant spectrum (Fig. 3b) because the local increase in electron temperature and safety factor alters the AE continuum [6].The background-subtracted fast-ion deuterium alpha (FIDA) density profiles at t=1030 ms show that higher fast-ion densities were reached with ECH (Fig. 3c-d), indicating that the critical gradient depends on the given experiment condition [2]. In Fig. 4a, large, transient spikes in the fast-ion loss detector disappeared when ECH was added. These intermittent losses are isolated, short lived (1-3 μs, on the order of several decay times of the scintillator), and are different than periodic loss signal amplitude variation due to beam-ion resonant-AE interactions. The spikes occur for specific time ranges in the current ramp, indicating a sensitive dependence on the equilibrium evolution. The spikes are largely reduced when ECH is added, which could be the effect of altered AE mode activity or different equilibrium, since the higher central electron temperature with ECH causes a delay in the current penetration to the axis, increasing the central safety factor profile inward from ρ_{qmin} (Fig. 4b). The amplitude of the spikes is much larger than the prompt loss beam ion signal and is approximately at discrete levels. One possibility is that the spikes are high energy charged fusion products, such as 3 MeV protons, 1 MeV tritons, or 0.8 MeV ^{3}He from primary D-D reactions. However, the large pitch required for the small gyroradius to enter the detector makes it unlikely that fusion products could physically collide with the FILD scintillator. Furthermore, the increased T_e in the ECH case creates more fusion reactions, but fewer losses are detected. Another possibility is sudden loss of a specific population of fast-ions during RSAE-TAE mode overlap. Further particle trajectory analysis is underway.

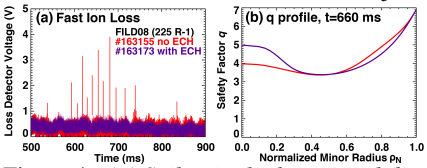

Figure 4: *(a) Spikes in the loss signal disappeared with ECH. (b) ECH raises q_0.*

III. Implications of Experiment Results for Reduced Model Development

A key research goal of energetic particle physics is to develop and validate reduced fast-ion transport models. One approach has been to use a "critical gradient" model, which assumes that if the fast-ion gradient ($\partial\beta_{EP}/\partial r$) exceeds a threshold either at or above the linear stability threshold of the fastest growing mode, fast ions are strongly transported by the AEs to flatten the profile and maintain marginal stability [7, 8]. In practice, critical gradient algorithms 1) use equilibrium profiles (n, T, B, etc.) to 2) calculate the AE spectrum and growth rates, 3) determine whether the critical gradient transport threshold is exceeded, and 4) adjust the fast ion gradient to force marginal stability. Regarding step 3, experiments show that the threshold is associated with multiple overlapping modes causing stochastic fast-ion orbits, although calculation of the stochastic transport threshold requires knowledge of mode amplitudes. The measured critical radial beam ion density gradient is specific to a given experimental condition, and recent experiments in negative triangularity plasmas show the critical gradient is higher compared to oval-shaped plasmas ($10.5 \times 10^{18}\mathrm{m}^{-4}$ vs $8 \times 10^{18}\mathrm{m}^{-4}$). Negative triangularity plasmas exhibit markedly lower microturbulence levels, providing an interesting test-case for models that predict higher critical gradient thresholds when background ITG/TEM turbulence is large. For step 4, current models calculate local growth rates and locally adjust the fast ion profile by a simple scaling factor. However, simulations using the kick model produce a hollow fast-ion profile that matches FIDA measurements [4], suggesting that AE structure extending near the core can drive substantial outward transport.

In conclusion, experimental results show that fast-ion transport varies in phase space, implying that treatment of AEs in phase space is important in accurately predicting density and current profiles. Ideally, a reduced fast-ion transport model would produce a phase-space diffusivity for input to TRANSP to calculate the fast-ion distribution, beam deposition, and expected data signals for predictive discharge modeling for burning plasma scenario development.

*Work supported by U.S. Department of Energy under DE-FC02-04ER54698, DE-FG03-94ER54271, and DE-AC02-09CH11466.

References

[1] C.S. Collins, W.W. Heidbrink, M.E. Austin, *et al.*, Phys. Rev. Lett. **116**, 095001 (2016)

[2] C.S. Collins, W.W. Heidbrink, M.Podestà, *et al.*, Nucl. Fusion **57**, 086005 (2017)

[3] W.W. Heidbrink, C.S. Collins, L. Stagner, *et al.*, Nucl. Fusion **56**, 112011 (2016)

[4] W.W. Heidbrink, C.S. Collins, M.Podestà, *et al.*, Phys. Plasmas **24**, 056109 (2017)

[5] M.Podestà, M. Gorelenkova, and R.B. White, Plasma Phys. Control. Fusion **56**, 055003 (2014).

[6] M.A. Van Zeeland, W.W. Heidbrink, S.E. Sharapov, *et al.*, Nucl. Fusion **56**, 112007 (2016).

[7] K. Ghantous, N. N. Gorelenkov, H. L. Berk, *et al.*, Phys. Plasmas **19**, 092511 (2012)

[8] R.E. Waltz and E.M. Bass, Nucl. Fusion **54**, 104006 (2014)